Influence of atomic density in high-order harmonic generation

Altucci, C; Starczewski, Tomas; Mevel, E; Wahlström, Claes-Göran; Carre, B; L'Huillier, Anne

Published in:
Optical Society of America. Journal B: Optical Physics

DOI:
10.1364/JOSAB.13.000148

1996

Influence of atomic density in high-order harmonic generation

C. Altucci,* T. Starczewski, E. Mevel, and C.-G. Wahlström

Department of Physics, Lund Institute of Technology, P.O. Box 118, S-221 00 Lund, Sweden

B. Carré and A. L'Huillier

Service des Photons, Atomes, et Molécules, Centre d'Etudes de Saclay, 91191 Gif-sur-Yvette, France

Received March 31, 1995; revised manuscript received July 3, 1995

We have investigated how high-order harmonics generated in rare gases depend on the atomic density. The peak and the profile of the atomic density in the interaction region were measured as a function of the backing pressure and the distance from the nozzle by a differential interferometry technique. The conversion efficiency for the harmonics in the plateau was found to increase approximately quadratically over the entire range of peak pressures investigated (3–80 mbar). The intensity of the harmonics in the cutoff region, in contrast, increased only until an optimum peak pressure was reached, beyond which it decreased. This optimum peak pressure was found to be dependent on both the laser intensity and the process order. To understand this effect, we have performed extensive propagation calculations of both the fundamental and the harmonic fields, using ionization rates and dipole moments from a tunnel ionization model. We obtained good agreement with the experimental results. The observed effect is attributed to ionization-induced defocusing of the fundamental laser beam, which reduces the peak intensity obtained in the medium and shortens the extent of the plateau. © 1996 Optical Society of America

1. INTRODUCTION

High-order harmonic generation by means of high-power lasers has been found to be a promising way of producing ultrashort pulses of intense, coherent radiation in the extreme ultraviolet and the soft-x-ray ranges. Harmonic orders as high as 143 and wavelengths as short as 7 nm[1–3] have been obtained by use of short-pulse lasers in the near infrared. In the high-intensity (10^{13}–10^{15} W/cm^2) low-frequency regime the harmonic spectra are characterized by a broad plateau of nearly constant conversion efficiency, followed by an abrupt cutoff. The radiation generated in this way has recently begun to be used in several applications. Experiments that use harmonics in solid-state physics[4] and in atomic and molecular spectroscopy[5–7] have been reported.

To utilize fully the potential of this new source, it is important to optimize the radiation with respect to various parameters. Much research has been devoted to understanding how the maximum photon energy may be optimized. A reasonably good understanding of this problem is now being approached. In the single-atom response, as shown by Krause *et al.*,[8] the width of the plateau varies as $I_p + 3U_p$, where I_p is the field-free ionization potential of the atom and U_p is the ponderomotive energy. U_p (eV) $= 9.33 \times 10^{-14} I\lambda^2$, where I is the laser intensity (W/cm^2) and λ is the laser wavelength (μm). The experimental results follow, at least qualitatively, the predictions of this cutoff law for the dependences on the laser intensity,[9] the pulse duration, and the wavelength,[10] as well as on the atomic species.[2] However, the maximum energy measured is found, in general, to be somewhat lower than the value given by the cutoff law. This result is attributed to propagation effects and, more precisely, in the experiment by Wahlström *et al.*,[9] to the geometrical phase mismatch induced by focusing.[11] Experiments have also been performed to plasmas of alkali–metal ions, which were created by the focusing of a laser on a solid alkali–metal target, with both a high-frequency[12] and a low-frequency[13] laser. The number of harmonics observed in the latter experiment was far below that expected according to the single-atom cutoff law. This effect was at least partly explained by the defocusing of the fundamental field, which reduced the effective intensity in the medium.[14]

In contrast, the optimization of the maximum conversion efficiency for a given harmonic has barely been tackled. Focusing conditions have been shown to affect the conversion efficiency considerably.[10,15] The number of photons is also optimized by the use of high-frequency lasers and heavy rare gases, but to the detriment of the spectral range, as shown by the cutoff law. A simple way to improve the conversion efficiency is to increase the atomic density in the interaction region. Harmonic generation is a coherent process, which is expected to vary as the square of the atomic density. However, several factors might alter this simple scaling, with some of them being present in a neutral medium and others being induced by the (partial) ionization of the medium. In particular, the dispersion in the neutral or in the partially ionized medium is expected to limit the quadratic dependence of the conversion efficiency with the atomic density. The role of the free-electron dispersion on the pressure dependence was recently pointed out by Rae *et al.*[16] in a theoretical study.

0740-3224/96/010148-09$06.00

The study of the dependence of the number of photons produced on pressure is thus important not only from a practical point of view, for optimizing the efficiency, but also for understanding the intrinsic limitations of the generation process. This consideration was the motivation for the present study. Preliminary experiments have been performed by Li *et al.*[17] with a 36-ps laser at 1.06 μm and by Rosman *et al.*[18] for the fifth harmonic by means of a 1-ps laser at 248 nm. The present research extends these investigations by systematically studying the influence of the atomic density at different laser intensities on high-order harmonic generation.

The experiments consisted of measuring the number of harmonics produced in a gas jet of Ne or Ar as a function of the backing pressure at which the pulsed valve, producing the atomic beam, is operated and for a given laser-nozzle distance. The laser used was the 150-fs terawatt laser of the Lund High-Power Laser Facility.[19] The main experimental difficulty was to characterize the atomic density in the interaction region (peak pressure and density profile), with sufficient time resolution, as a function of the backing pressure and the distance between the laser focus and the nozzle. This characterization was achieved with a differential interferometric technique.[20] To interpret our experimental results we performed systematic propagation calculations in an ionizing gas for both the fundamental and the harmonic fields.[21] We used ionization rates and dipole moments deduced from the approach developed by Lewenstein *et al.*[22], which is valid in the tunnel ionization limit.

In Section 2 we describe the experimental method. The gas jet diagnostics and the results concerning the jet characterization are presented in Sections 3 and 4, respectively. The experimental pressure studies and the numerical simulations are presented in Sections 5 and 6, respectively. In Section 7 we discuss the interpretation of our results. Finally, in Section 8, we summarize and present the conclusions drawn from this study.

2. LASER SYSTEM AND EXPERIMENTAL ARRANGEMENT

The laser used was a Ti:sapphire laser system based on chirped pulse amplification, with a 150-fs pulse duration, a 10-Hz repetition rate, and a pulse energy of up to 220 mJ.[19] In the present experiment we operated the laser at a fixed wavelength of 795 nm. To obtain a well-defined spatial mode and to optimize the conversion efficiency, we apertured the 50-mm beam to 25 mm before it was focused by a plano-convex lens ($f = 1.0$ m). The maximum pulse energy entering the vacuum chamber in which the harmonics were generated was limited to 30 mJ. In the present experiment we did not measure the focal spot but determined the laser intensity by comparing harmonic intensity dependences with similar ones obtained in a previous experiment.[9]

The vacuum system and the spectrometer used to generate and to detect the harmonics were described by Wahlström *et al.*[9] The nozzle used to produce the gas jet is described in Section 3. The spectrometer consists of a toroidal mirror and a plane grating (700 grooves/mm). To optimize the throughput, no entrance slit was used. Finally, the harmonics were detected with an electron multiplier and were recorded with a computer-based data-acquisition system.

3. GAS JET DIAGNOSTICS

The pulsed nozzle[23] that we used and characterized is the one used in all the harmonic-generation experiments performed by the Saclay group since 1988. The valve is an injector-type device operated by a solenoid. The gas flows through a 6-mm tube with a 0.9-mm inner diameter. The current through the solenoid, which opens the valve, is on for typically 250 μs, approximately 750 μs before the laser pulse. These times, given by the dynamics of the valve and by the kinetics of the gas, are chosen to allow the gas to reach its maximum flow and to minimize the gas inlet into the vacuum system at the same time.

To characterize the gas jet under conditions similar to those under which harmonics are normally generated, the diagnostic technique must provide good spatial and temporal resolution simultaneously. The method used in this study is based on optical interferometry and is an extension of a technique developed for static gas-flow diagnostics.[20] It allows us to measure both the gas density and the spatial distribution of the jet as a function of the backing pressure and the distance from the nozzle orifice, with sufficient temporal resolution.

A schematic layout of the setup for gas diagnostics is shown in Fig. 1. A horizontal parallel sheet (20 mm $\times$ 0.5 mm) of light from a continuous He–Ne laser, polarized at 45° from the vertical axis, is sent through the gas jet. This sheet of light is viewed as an infinite number of parallel rays traveling through the medium. Each ray experiences a phase shift proportional to the integrated refractive index (given by the gas density distribution) along its path. The orthogonally polarized components of rays separated by a distance Δx during the passage of the gas are superimposed in a birefringent calcite crystal placed beyond the gas jet. We achieved this superimposition by orienting the optical axis of the crystal along the vertical axis and turning the crystal an angle θ in the horizontal plane. The crystal used was 20 mm long in the direction of the light propagation and was polished to $\lambda/5$ flatness. Finally, we obtained an interference pattern by making the superimposed rays pass through a polarizer oriented at 45° to the vertical axis and imaged onto a detector. Each set of parameters (backing pressure, distance from nozzle orifice, and gas species) requires the acquisition of three interference patterns: one with the gas jet present, one with the gas turned off, and one with the gas turned off and the final polarizer rotated 90°. These three intensity distributions together yield a corrected intensity distribution that approaches the gradient of the

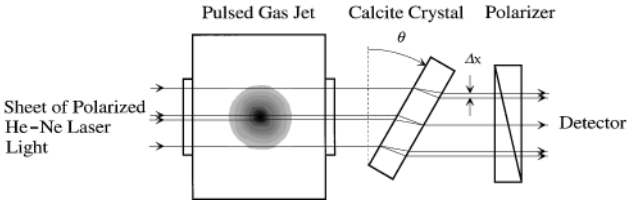

Fig. 1. Schematic showing the principle of the interferometric technique used for gas jet diagnostics.

path-integrated refractive index[20] as $\Delta x \to 0$. The sensitivity of the interferometer depends on the displacement Δx and is varied by means of a change in the tilt angle θ of the crystal. On the one hand, a θ value that is as small as possible should be chosen, as the final interference pattern will then approach the derivative limit. On the other hand, a small angle results in a small difference in the path-integrated refractive index for the interfering paths and consequently in a low detector signal and a low signal-to-noise ratio. Values of θ that are too large can cause systematic errors owing to the finite size of Δx and may also, in the general case, cause fringe ambiguity. In our experiment the total integrated phase shifts were very small (less than $\pi/20$), and we used a Δx value of 200 μm.

As the method was originally used for static gas flows, it was necessary to meet additional requirements on the detection system to work with a pulsed jet. First, the detector must be properly triggered in time (in our case, 1 ms after the start of the solenoid pulse). Second, the detection time must be short enough to match the dynamics of the gas pressure evolution (here of the order of tens of microseconds). This requirement rules out ordinary photodiode arrays, which have typical readout times of tens of milliseconds. A good dynamic range ($>10^3$) also has to be guaranteed because of the high level of background light. The ideal choice should be a gated array detector. However, we did not have access to such a detector at the time of the experiment and instead used a single photodiode on a translation stage, along with a digital oscilloscope.

The final intensity distribution was numerically integrated to yield the phase shift as a function of the space coordinate transverse to the laser axis. Then, assuming cylindrical symmetry in the jet and using an Abel-inversion algorithm,[24] we obtained the gas density distribution. The uncertainty in the experimental density values is estimated to be approximately $\pm 20\%$.

4. RESULTS OF THE GAS JET CHARACTERIZATION

All the spatial profiles of the gas distributions showed smooth, Lorentzian-like shapes except in the wings, where the experimental profiles were steeper (see Fig. 2). There was no significant dependence on the gas species used; Ar and Ne, at the same backing pressure, gave the same peak pressures and the same pressure profiles.

The normalized spatial profile, measured at a given distance below the nozzle orifice, was found to be almost independent of the backing pressure within our experimental range of peak pressures (3–80 mbar). There was only a small widening of the profile with increasing pressure. The peak pressure, at a fixed distance from the orifice, increased almost linearly as a function of the backing pressure, as shown in Fig. 3. The small nonlinearity corresponds to the widening of the spatial distribution with increasing pressure. The pressure values obtained are in agreement (within a factor of 2) with measurements of the same gas jet made by a technique based on laser-induced fluorescence.[23]

The peak pressure and the width of the jet were investigated as a function of the distance h from the nozzle orifice. The pressure was found to decrease with increasing distance approximately as $(h_0 + h)^{-2}$, whereas the width of the profile, measured at half-maximum, increased linearly with the distance. The full divergence angle increased from 30° at the lowest to 40° at the highest backing pressure. These findings are in good agreement with each other and with the requirement of conservation of flow (see Fig. 4).

5. EXPERIMENTAL RESULTS

First we discuss the results obtained in Ne for the spectral region close to the cutoff. In Fig. 5 we show harmonic spectra obtained at several peak pressures (7, 30, and 80 mbar). The intensity was estimated to be 10^{15} W/cm^2. The nozzle–focus distance was 0.5 mm, for which the length of the medium [i.e., its full width of half-maximum (FWHM)] was 1.2 mm. The spectra were normalized to 1 at the 51st harmonic. The cutoff region is considerably affected by the peak pressure. At the highest peak pressure the harmonic intensity falls rapidly

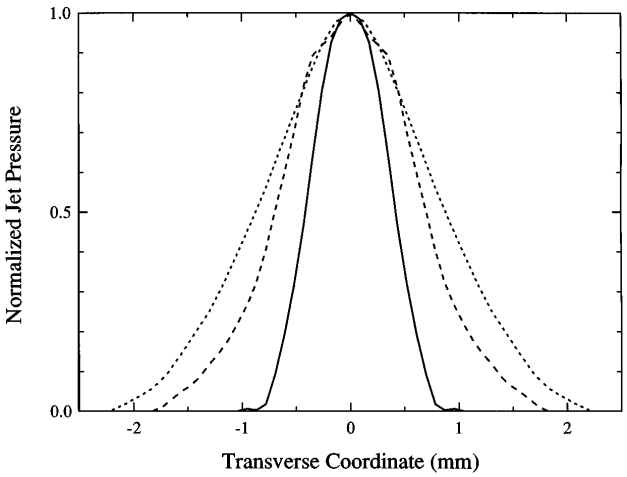

Fig. 2. Normalized density profiles at three different laser-nozzle distances: 0 (solid curve), 0.75 mm (dashed curve), and 1.2 mm (dotted curve). The backing pressure was adjusted to yield the same peak pressure (27 mbar) at the different distances.

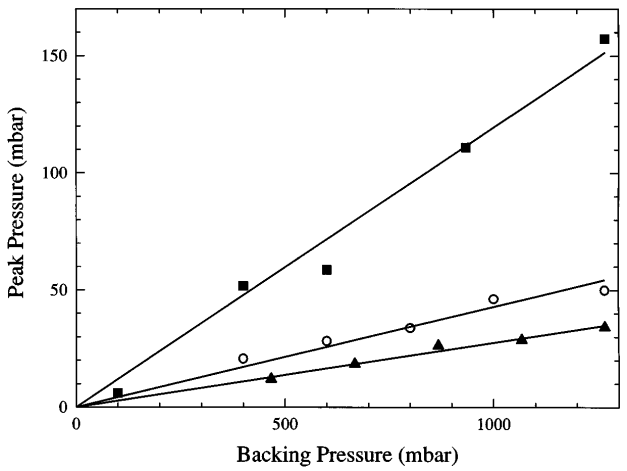

Fig. 3. Peak pressure as a function of backing pressure at three laser-nozzle distances: 0 (squares), 0.75 mm (circles), and 1.2 mm (triangles).

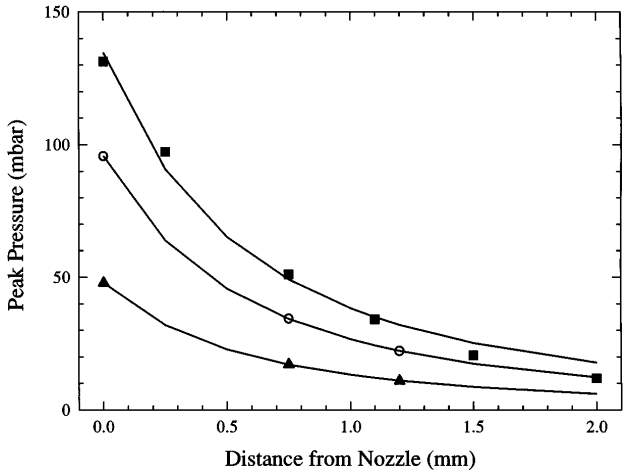

Fig. 4. Peak pressure as a function of the distance from the nozzle. The backing pressures were 1270 mbar (squares), 800 mbar (circles), and 600 mbar (triangles).

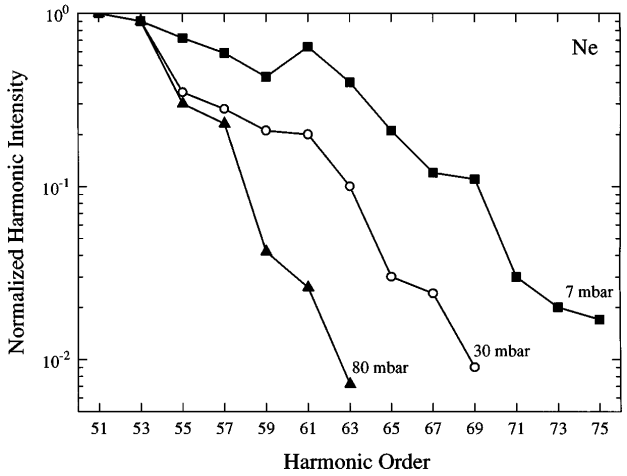

Fig. 5. Harmonic spectra in the cutoff region in Ne at three different peak pressures: 7, 30, and 80 mbar.

beyond the 55th order, whereas at the lowest pressure harmonics can be seen until the 75th order.

To understand this effect better, we systematically studied the dependence of the harmonic intensity on the peak pressure. The results are presented in Figs. 6 and 7 at two intensities, 6×10^{14} W/cm^2 and 1.5×10^{15} W/cm^2, respectively. Each pressure point (indicated by the filled circles in Figs. 6 and 7) is an average of 100 shots, all with pulse energies within $\pm 15\%$ of a set value. In the plateau region (harmonics below the 55th), the number of photons increased as the square of the atomic density over the range investigated (3–80 mbar). In the cutoff region the harmonic yield goes through a maximum and then decreases. The pressure corresponding to this maximum decreases as the process order increases. Moreover, for a given harmonic order, this optimum pressure increases with the laser intensity. In Fig. 7 we show (dotted curve at the bottom) the pressure dependence of the background recorded at 11 nm, i.e., between the 71st and the 73rd harmonics. First it increases with pressure (again quadratically); then it saturates. The origin of the background is not clear. It might be due partly to the overlap between two consecutive harmonics (which are quite broad) and partly to scattering by the grating of intense, low-order, harmonics. It decreases slightly with decreasing wavelength, so that the 75th and the 77th harmonics shown in Fig. 7 are actually just above the background level at low pressure. In Fig. 8 we show the 67th harmonic as a function of the pressure at several laser intensities from 6×10^{14} W/cm^2 to 1.5×10^{15} W/cm^2. The pressure points are indicated by filled circles. The optimum pressure increase with the laser intensity is clearly shown.

The same effect, i.e., the reduction of the extent of the plateau at high pressure, was also observed in Ar. We show in Fig. 9 harmonic spectra obtained at different pressures (10 and 60 mbar). The intensity used in this series of measurements was quite high, 4×10^{14} W/cm^2, above the saturation intensity for ionization. In addition to the effect of the pressure on the harmonics of the cutoff region, the harmonic lines are clearly blue shifted and broadened.[9,16] Figure 10 shows the spectral profiles of the 21st harmonic, taken with a higher resolution, at different pressures. Note that, for the case of higher harmonics in Ne, this effect could not be observed because

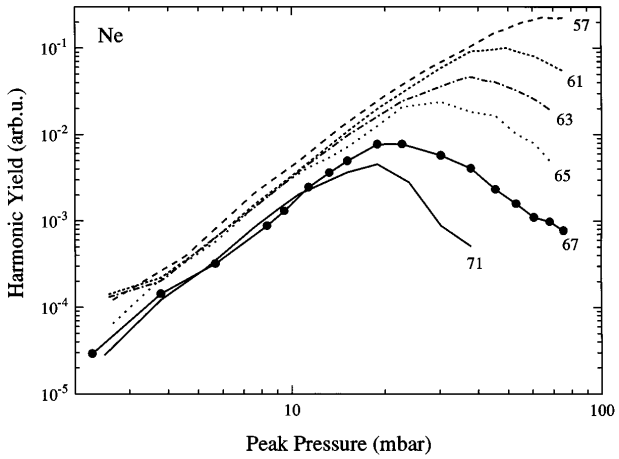

Fig. 6. Number of photons at different harmonic frequencies (from the 57th, at the end of the plateau, to the 71st, in the cutoff) as a function of pressure. The laser intensity was 6×10^{14} W/cm^2.

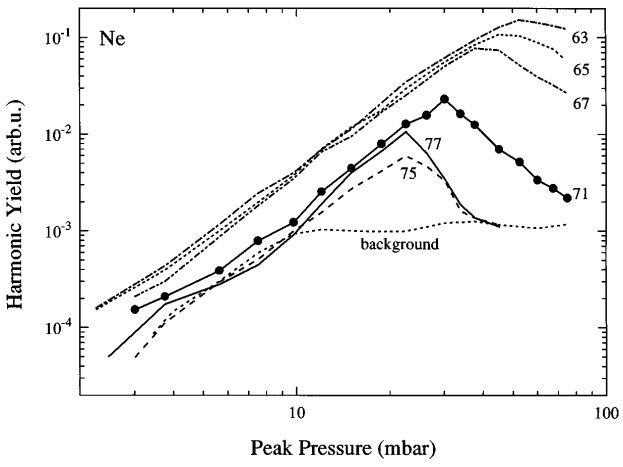

Fig. 7. Same as Fig. 6, but at a higher laser intensity (1.5×10^{15} W/cm^2). The background level is indicated by the dotted curve at the bottom.

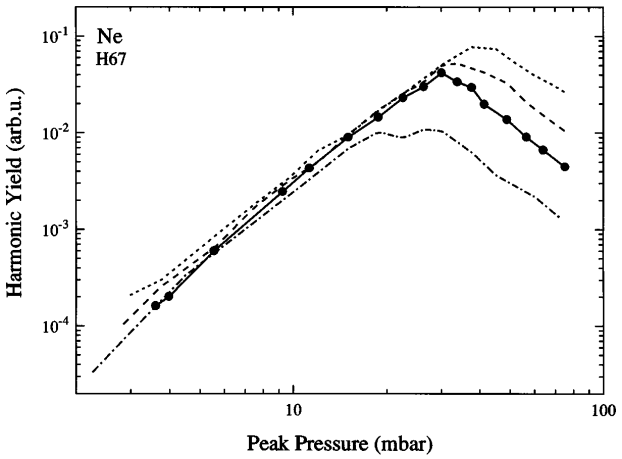

Fig. 8. Number of photons at the 67th harmonic frequency as a function of pressure, at different laser intensities (6, 7.5, 10, 15×10^{14} W/cm^2, from the bottom curve to the top curve, respectively).

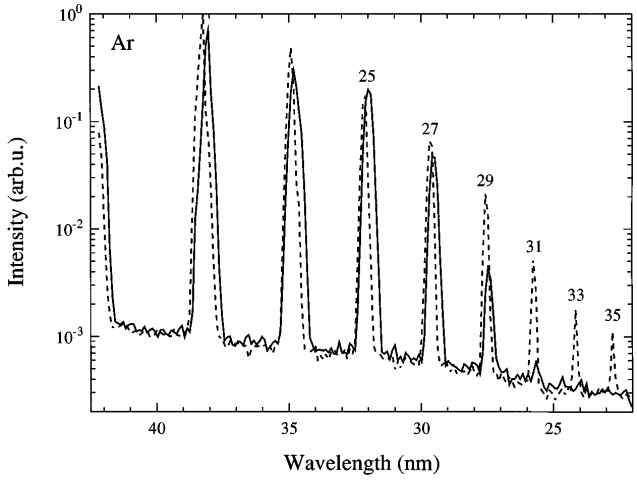

Fig. 9. Normalized harmonic spectra in Ar at 10 mbar (dashed curve) and 60 mbar (solid curve). The laser intensity was 4×10^{14} W/cm^2.

the linewidths of the harmonics were smaller than the instrumental resolution (approximately 0.5 Å). For all the harmonics generated in Ar, including those in the plateau region, the dependence on the pressure was found to deviate from the quadratic behavior for pressures beyond 16 mbar. This result is illustrated in Fig. 11 for the 21st harmonic. The harmonic yields are calculated in this case by integration of the spectral profile, to account for the blue shift.

Finally, we also studied the dependence of the harmonic efficiency on the length of the medium. We did this simply by varying the laser-nozzle distance and by keeping the peak pressure constant, relying on the characterization described in Section 4. The width of half-maximum varied from 0.8 mm to approximately 2.4 mm when the laser-nozzle distance increased from 0 to 2 mm. We observed very little influence of the length of the medium on the efficiency, as shown in Fig. 12 for several harmonics generated in Ar.

6. NUMERICAL SIMULATIONS

Because the interpretation of our experiments is, to a large extent, based on extensive numerical simulations, we now describe in some detail our approach to the theoretical description of harmonic-generation processes. Two steps are necessary: the calculation of the single-atom emission spectrum, and the solution of the propagation equation for the fundamental and the generated fields in the nonlinear medium. The calculation of the amplitude and the phase of the dipole moment for each harmonic frequency is achieved by use of the formulation developed by Lewenstein and co-workers,[22] which is valid for high intensities and low frequencies in the tunneling limit. The atomic description is quite crude (the contribution of bound states is neglected), but the dynamics of the electron in the laser field is well described. This model was shown to be quite realistic in several calculations.[11,25] The second step of the theoretical description consists of solving the propagation equations in the slowly varying envelope approximation,[21] using these dipole moments as source terms. The ionization of the medium is taken into account, with tunnel ionization rates calculated by the method of Lewenstein *et al.*[22]

The approximations used for solving the propagation equations are described in detail in L'Huillier *et al.*[21]

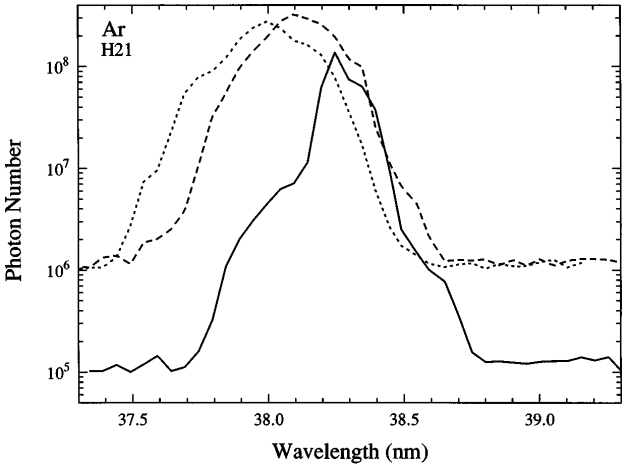

Fig. 10. Pressure-dependent blue shift and blue broadening for the 21st harmonic generated in Ar at 7×10^{14} W/cm^2. The peak pressures were 5 mbar (solid curve), 45 mbar (dashed curve), and 80 mbar (dotted curve).

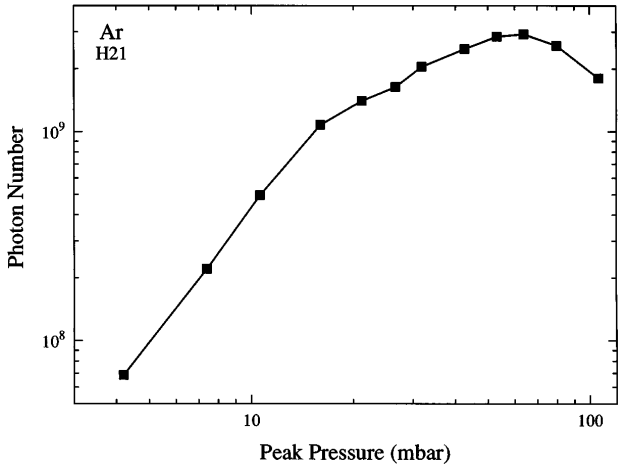

Fig. 11. Number of photons at the 21st harmonic frequency as a function of pressure. The laser intensity was 4×10^{14} W/cm^2. The squares indicate the experimental points.

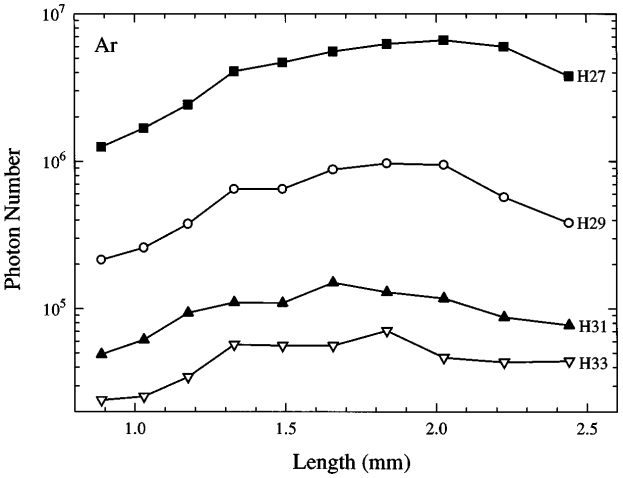

Fig. 12. Number of photons at different harmonic frequencies in Ar as a function of the length of the medium. The laser intensity was 7×10^{14} W/cm^2; the peak pressure, 14 mbar.

Briefly, we first solve the propagation equation for the fundamental field E_1 (cgs units):

$$\nabla_\perp^2 E_1 + 2ik_1 \frac{\partial E_1}{\partial z} + 2k_1 \delta k_1 E_1 = 0\,, \tag{1}$$

where k_1 denotes the wave vector and δk_1 denotes the intensity-dependent correction to the wave vector induced by the free electrons.

$$\delta k_1(r, z, t) = -2\pi e^2 \mathcal{N}_e(r, z, t)/m\omega c\,, \tag{2}$$

where e, m are the charge and the mass of the electron, respectively; c is the velocity of light; ω, the laser frequency; and $\mathcal{N}_e$, the local electron density, assumed to be equal to the local ion density (the electrons are frozen during the laser pulse). Equation (1) is nonlinear because the electron density depends on $|E_1(r, z, t)|^2$.

Next we calculate the nonlinear polarization P_q induced by the perturbed fundamental field E_1. Then we solve the propagation equation for the harmonic field E_q:

$$\nabla_\perp^2 E_q + 2ik_q \frac{\partial E_q}{\partial z} + 2k_q(\delta k_q + \Delta k_q)E_q = -4\pi(q\omega/c)^2 P_q\,. \tag{3}$$

Here δk_q denotes the contribution of the free electrons to the wave vector at the qth harmonic frequency k_q. The effect of δk_q $(=\delta k_1/q)$ is much smaller than the effect of δk_1 on the fundamental, which leads to a phase factor $q\delta k_1$ on the polarization at frequency $q\omega$. Δk_q (which can be complex) denotes the phase mismatch induced by the atoms (or ions) in the medium; its imaginary part is the absorption coefficient.

The propagation equations (1) and (3) are solved numerically over the length of the nonlinear medium by finite-difference techniques. They are discretized in the (r, z) plane on a 500×300 point grid and are integrated by a space-marching Crank–Nicholson scheme. This integration is repeated for a sequence of times t spanning the laser-pulse duration (typically 100 points). We obtain the photon yield by integrating, in the transverse direction and in time, the intensity of the harmonic field at the exit of the medium.[21] We try to reproduce the experimental conditions. The 795-nm-wavelength laser is assumed to be Gaussian in space and time, with a 5-mm confocal parameter and a 150-fs pulse duration. The generating gas is Ne, and the atomic density profile is a truncated Lorentzian function with a 1.2-mm FWHM (for a laser-nozzle distance of 0.5 mm). The Lorentzian function is truncated at $z = \pm 1.2$ mm. The total length of the medium is therefore twice the width at half-maximum. The dimension of the grid in space is 100 μm $\times$ 2.4 mm; in time, 500 fs. We consider relatively high-order harmonics from the 55th to the 75th.

We find that in these conditions the influence of the atomic (or ionic) phase mismatch remains negligible compared with the contribution of the free electrons. Absorption remains weak in Ne or Ne^+, for the pressures, the interaction length, and the high photon energies considered in the present study, as is discussed in Section 7. The numerical simulations presented below were obtained by consideration of only the effect of the free electrons.

In Fig. 13 we show numerical results obtained for the 63rd, the 67th, and the 75th harmonics at an intensity of 8×10^{14} W/cm^2. The theoretical results show the same saturation effect and approximately the same order-dependent optimum pressure as in the experiments. The results are almost identical to those shown in Fig. 7, but for a lower intensity. In Fig. 14 we show the variation in the 67th harmonic with pressure at several laser intensities (6, 7, 8, 9×10^{14} W/cm^2 from the bottom curve to the top curve, respectively). This set of curves resembles the experimental evolution shown in Fig. 8.

To reproduce the saturation observed in the experiments, it was essential to calculate accurately the distortion of the fundamental field and, in particular, the defocusing due to the spatial gradient of the refractive index induced by the free electrons.[14,26] If we neglect the defocusing effect, and more precisely the radial variation of δk_1, Eq. (1) can be solved analytically, and Eq. (3) becomes

$$\nabla_\perp^2 E_q + 2ik_q \frac{\partial E_q}{\partial z} + 2k_q(\delta k_q - q\delta k_1)E_q = -4\pi(q\omega/c)^2 P_q\,, \tag{4}$$

where P_q is now induced by the nonperturbed fundamen-

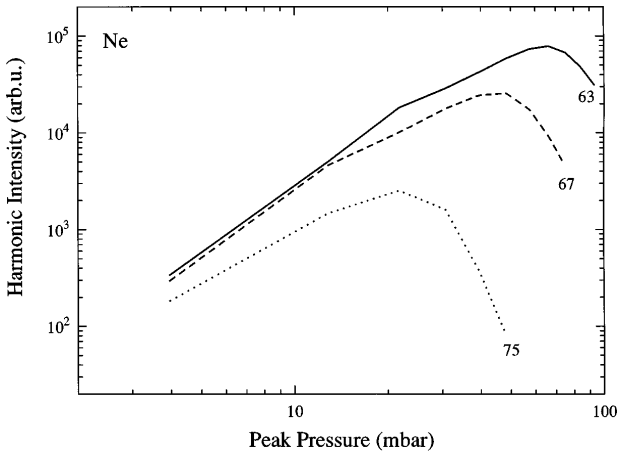

Fig. 13. Theoretical number of photons at the 63rd, the 67th, and the 75th harmonic frequencies as a function of pressure.

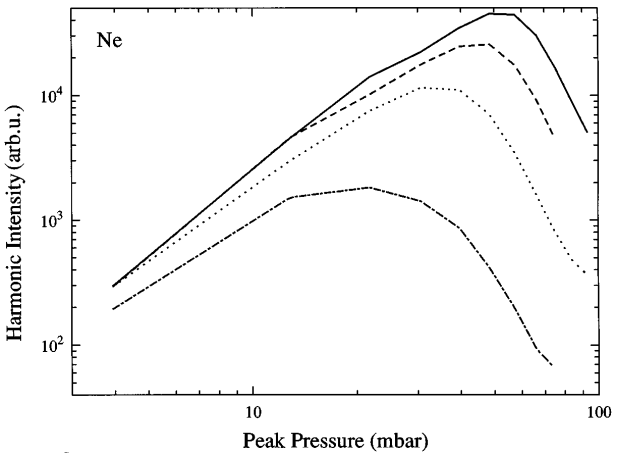

Fig. 14. Theoretical number of photons at the 67th harmonic frequency as a function of pressure at different laser intensities: 6, 7, 8, 9×10^{14} W/cm^2, from the bottom curve to the top curve, (see Fig. 8 for comparison).

tal field (we have also set $\Delta k_q = 0$). This equation takes into account the phase mismatch ($\delta k_q - q\delta k_1$) induced by the free electrons, but not the defocusing effect. We show in Fig. 15 results obtained by solving of Eq. (4) instead of Eqs. (1) and (3). They were obtained under the same conditions as in Fig. 13, except that defocusing is not taken into account. Similar calculations were performed by Rae *et al.*,[16] who also found a saturation induced by the free-electron dispersion. However, the decrease observed experimentally is not reproduced in this calculation, which neglects the radial dependence of the refractive index. This result leads us to the natural conclusion that the decrease observed in the experimental results is due to defocusing of the fundamental field in the partially ionized medium.

7. INTERPRETATION OF THE EXPERIMENTAL RESULTS

We now discuss the different pressure-dependent effects that might induce a deviation of the quadratic dependence of the harmonic-generation conversion efficiency on the atomic density.

The single-atom response itself might be affected. High-order harmonic generation in the low-frequency high-intensity regime can be understood as a two-step process[27]: electrons tunnel out through the atomic potential, oscillate in the laser field, and can come back toward the nucleus with a high kinetic energy, producing high-order harmonics. The quiver amplitude of an electron exposed to an intensity of 10^{15} W/cm^2 at 800 nm is 2.8 nm. At the highest pressure used in our experiment, 80 mbar ($\approx 2 \times 10^{18}$ atoms/cm^3), the average distance between two atoms is 8 nm, i.e., only a factor of 3 higher than the quiver amplitude. One could therefore expect the return of the electron toward the nucleus to be disturbed by the presence of other atoms. Although this effect cannot be ruled out, the fact that the numerical simulations reproduce the experimental results without taking it into account is a strong indication that it plays only a minor role, if any, in this process.

The phase mismatch introduced by dispersion, as well as reabsorption, are pressure-dependent effects that could limit the conversion efficiency. Let us first examine the influence of reabsorption. Consider, for example, the 67th harmonic, which corresponds to a photon energy of 104 eV. The photoionization cross section[28] of Ne at 104 eV is 3.3 Mb. The absorption coefficient κ_q at 80 mbar is thus 3.3 cm^{-1}. This means that approximately 50% of the radiation has been absorbed over the medium's length at the highest pressure used (80 mbar). This number overestimates the effect, since it assumes that the medium is not depleted by ionization (Ne^+ has a smaller photoionization cross section). The effect observed in the experiment is much more pronounced than this factor-of-2 reduction.

Under the conditions considered in the present study, high-order harmonic generation is always accompanied by partial ionization of the medium. The presence of free electrons that are due to ionization of the medium introduces a substantial phase mismatch between the generated field and the driving nonlinear polarization. The atomic phase mismatch is in general negligible compared with that induced by the free electrons,[29] especially for high-order harmonics, because the latter contribution, $-q\delta k_1$, is proportional to the harmonic order q. Moreover, these electrons can give rise to significant defocusing[14,26] as well as spectral blue shifting[9,16] of the fundamental field. The simulations presented in Section 6 show that the main effect responsible for the saturation and the decrease of the harmonic efficiency as a function of pressure appears to be the defocusing of the fundamental field.

For illustration purposes we show in Fig. 16 a three-dimensional picture of the fundamental field in the partially ionized nonlinear medium, at a fixed time, toward the end of the laser pulse. $|E_1(r, z - ct)|$ is represented as a function of r and z, over 100 μm and 2.4 mm. The maximum pressure is 70 mbar, and the peak intensity in vacuum is 7×10^{14} W/cm^2. The effective medium, over which the intensity remains significant, is significantly reduced. The maximum intensity in the medium is very close to the intensity at the entrance of the nonlinear medium (and at the maximum of the laser pulse) because the beam immediately starts to defocus. Owing to the collimated geometry and the short medium length, this

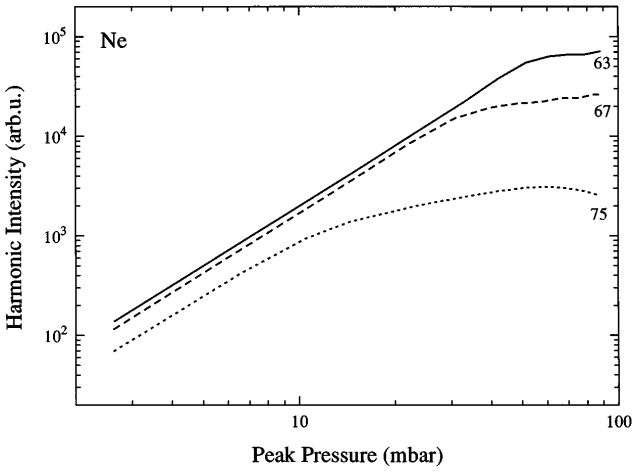

Fig. 15. Theoretical number of photons at the 63rd, the 67th, and the 75th harmonic frequencies as a function of pressure without taking into account defocusing.

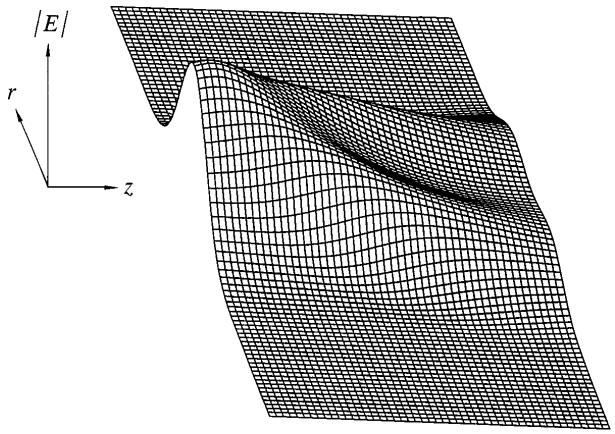

Fig. 16. Illustration of ionization-induced defocusing of the fundamental laser pulse as it propagates through the partially ionized medium.

maximum intensity, reached at $z = -1.1$ mm (with the medium being between ± 1.2 mm), is 5.8×10^{14} W/cm^2. The region of maximum intensity is therefore right at the entrance of the medium, where the atomic density is reduced. In vacuum the intensity variation over the medium length (2.4 mm) is approximately 18%, owing to the collimated geometry. The same intensity variation occurs now over a much more reduced length (0.6 mm at the maximum of the laser pulse).

The above arguments allow us to understand why the optimum pressure observed experimentally depends on the process order and laser intensity and is higher for the harmonics in the plateau. The harmonics in the cutoff region are produced at the highest intensity and are strongly reduced as the intensity in the medium and the effective interaction length decrease. In contrast, the harmonics in the plateau are produced also at lower intensities, and consequently over a large volume and at the beginning of the pulse, for which the defocusing of the fundamental is not as important. Therefore the conversion efficiency for these harmonics is not affected so much by the defocusing of the fundamental.

The refraction effect might also explain why the harmonic yield seems to be only weakly dependent on the medium's length (as shown in Fig. 12), which is obtained at a relatively high pressure (14 mbar). Note, however, that the interpretation of this result requires a comparison between the coherence length of the process, which is imposed both by propagation and by the atomic dipole phase,[25] and the effective medium length. Additional systematic experimental studies, as well as numerical simulations, which go beyond the scope of the present paper, would be required for understanding how the harmonic yield depends on the length of the atomic medium.

8. SUMMARY AND CONCLUSIONS

In this study we have examined experimentally the dependence of high-order harmonic generation on the atomic density. The pulsed gas jets has been characterized with an interferometric technique, providing good temporal resolution. The results show that the quadratic dependence of the conversion efficiency with the atomic density is valid up to a maximum pressure, which depends on the gas, the intensity, and the process order. This limitation is interpreted with the aid of numerical simulations as ionization-induced defocusing of the fundamental field. This defocusing affects harmonic generation differently, depending on whether the harmonic is in the plateau region or in the cutoff region. In particular, the maximum photon energy reached depends on the atomic pressure used in the experiment.

ACKNOWLEDGMENTS

We thank A. Persson for valuable help with the optimization of the laser and P. Salières and M. Lewenstein for their help with the theoretical interpretation. We acknowledge the support of the Swedish Natural Science Research Council, the Direction des Recherches, Etudes et Techniques under contract 92-439, and the European Community Human Capital and Mobility Programme.

*Present address, Dipartimento di Scienze Fisiche, Università di Napoli, Naples, Italy.

REFERENCES

1. J. J. Macklin, J. D. Kmetec, and C. L. Gordon III, "High-order harmonic generation using intense femtosecond pulses," Phys. Rev. Lett. **70,** 766 (1993).
2. A. L'Huillier and Ph. Balcou, "High-order harmonic generation in rare gases with a 1-ps 1053-nm laser," Phys. Rev. Lett. **70,** 774 (1993).
3. M. D. Perry and G. Mourou, "Terawatt to petawatt subpicosecond lasers," Science **264,** 917 (1994).
4. R. Haight and D. R. Peale, "Antibonding state on the Ge(111):As surface: spectroscopy and dynamics," Phys. Rev. Lett. **70,** 3979 (1993); "Tunable photoemission with harmonics of subpicosecond lasers," Rev. Sci. Instrum. **65,** 1853 (1994); R. Haight and P. F. Seidler, "High resolution atomic core level spectroscopy with laser harmonics," Appl. Phys. Lett. **65,** 517 (1994).
5. Ph. Balcou, P. Salières, K. S. Budil, T. Ditmire, M. D. Perry, and A. L'Huillier, "High-order harmonic generation in rare gases: a new source in photoionization," Z. Phys. D **34,** 107 (1995).
6. J. Larsson, E. Mevel, R. Zerne, A. L'Huillier, C.-G. Wahlström, and S. Svanberg, "Two-colour time-resolved spectroscopy of helium using high-order harmonics," J. Phys. B **28,** L53 (1995).
7. P. Erman, A. Karawajczyk, E. Rachlew-Källne, E. Mevel, R. Zerne, A. L'Huillier, and C.-G. Wahlström, "Autoionization widths of the NO Rydberg-valence state complex in the 11–12 eV region," Chem. Phys. Lett. **239,** 6 (1995).
8. J. L. Krause, K. J. Schafer, and K. C. Kulander, "High-order harmonic generation from atoms and ions in the high intensity regime," Phys. Rev. Lett. **68,** 3535 (1992).
9. C.-G. Wahlström, J. Larsson, A. Persson, T. Starczewski, S. Svanberg, P. Salières, Ph. Balcou, and A. L'Huillier, "High-order harmonic generation in rare gases with an intense short-pulse laser," Phys. Rev. A **48,** 4709 (1993).
10. Ph. Balcou, C. Cornaggia, A. S. L. Gomes, L. A. Lompré, and A. L'Huillier, "Optimizing high-order harmonic generation in strong fields," J. Phys. B **25,** 4467 (1992).
11. A. L'Huillier, M. Lewenstein, P. Salières, Ph. Balcou, M. Yu. Ivanov, J. Larsson, and C.-G. Wahlström, "High-order harmonic generation cutoff," Phys. Rev. A **48,** R3433 (1993).
12. Y. Akiyama, K. Midorikawa, Y. Matsunawa, Y. Nagata, M. Obara, H. Tashiro, and K. Toyoda, "Generation of high-order harmonics using laser-produced rare-gas-like ions," Phys. Rev. Lett. **69,** 2176 (1992).
13. C.-G. Wahlström, S. Borgström, J. Larsson, and S.-G. Pettersson, "High-order harmonic generation in laser-produced ions using a near infrared laser," Phys. Rev. A **51,** 585 (1995).

14. S. C. Rae, "Ionization-induced defocusing of intense laser pulses in high-pressure gases," Opt. Commun. **97,** 25 (1993).
15. L.-A. Lompré, A. L'Huillier, P. Monot, M. Ferray, G. Mainfray, and C. Manus, "High-order harmonic generation in xenon: intensity and propagation effects," J. Opt. Soc. Am. B **7,** 754 (1990).
16. S. C. Rae, K. Burnett, and J. Cooper, "Generation and propagation of high-order harmonics in a rapidly ionizing medium," Phys. Rev. A **50,** 3438 (1994).
17. X. F. Li, A. L'Huillier, M. Ferray, L.-A. Lompré, and G. Mainfray, "Multiple-harmonic generation in rare gases at high laser intensity," Phys. Rev. A **39,** 5751 (1989).
18. R. Rosman, G. Gibson, K. Boyer, H. Jara, T. S. Luk, I. A. McIntyre, A. McPherson, J. C. Solem, and C. K. Rhodes, "Fifth-harmonic production in neon and argon with picosecond 248-nm radiation," J. Opt. Soc. Am. B **5,** 1237 (1988).
19. S. Svanberg, J. Larsson, A. Persson, and C.-G. Wahlström, "Lund High-Power Laser Facility—systems and first results," Phys. Scr. **49,** 187 (1994).
20. G. W. Faris and H. M. Hertz, "Tunable differential interferometer for optical tomography," Appl. Opt. **28,** 4662 (1989).
21. A. L'Huillier, Ph. Balcou, S. Candel, K. J. Schafer, and K. C. Kulander, "Calculations of high-order harmonic generation processes in xenon at 1064 nm," Phys. Rev. A **46,** 2778 (1992).
22. M. Lewenstein, Ph. Balcou, M. Yu. Ivanov, A. L'Huillier, and P. Corkum, "Theory of high-harmonic generation by low-frequency laser fields," Phys. Rev. A **49,** 2117 (1994).
23. L. A. Lompré, M. Ferray, A. L'Huillier, X. F. Li, and G. Mainfray, "Optical determination of the characteristics of a pulsed-gas jet," J. Appl. Phys. **63,** 1791 (1988).
24. C. Fleurier and J. Chapelle, "Inversion of Abel's integral equation—application to plasma spectroscopy," Comp. Phys. Commun. **7,** 200 (1974).
25. P. Salières, A. L'Huillier, and M. Lewenstein, "Coherence control of high-order harmonics," Phys. Rev. Lett. **74,** 3776 (1995).
26. P. Monot, T. Auguste, L. A. Lompré, G. Mainfray, and C. Manus, "Defocusing effects of a picosecond terawatt laser pulse in an underdense plasma," Opt. Commun. **89,** 145 (1992).
27. P. B. Corkum, "Plasma perspective on strong-field multiphoton ionization," Phys. Rev. Lett. **71,** 1994 (1993); see also K. C. Kulander, K. J. Schafer, and J. L. Krause, "Dynamics of short-pulse excitation, ionization and harmonics conversion," in *Super-Intense Laser-Atom Physics*, B. Piraux, A. L'Huillier, and K. Rzążewski, eds., NATO Advanced Science Institutes Series B: Physics (Plenum, New York, 1993), Vol. 316, p. 95.
28. W. F. Chan, G. Cooper, X. Guo, and C. E. Brion, "Absolute optical oscillator strengths for the electronic excitation of atoms at high resolution. II. The photoabsorption of neon," Phys. Rev. A **45,** 1420 (1992).
29. A. L'Huillier, X. F. Li, and L. A. Lompré, "Propagation effects in high-order harmonic generation in rare gases," J. Opt. Soc. Am. B **7,** 527 (1990).